

Electronic Supplementary Information

Insight into through-space conjugation in rotation-restricted thermally activated delayed fluorescence compounds

Kuofei Li, Yuannan Chen, Bing Yao, Kunkun Dou, Tao Wang, Hao Deng, Hongmei Zhan,* Zhiyuan Xie, Yanxiang Cheng

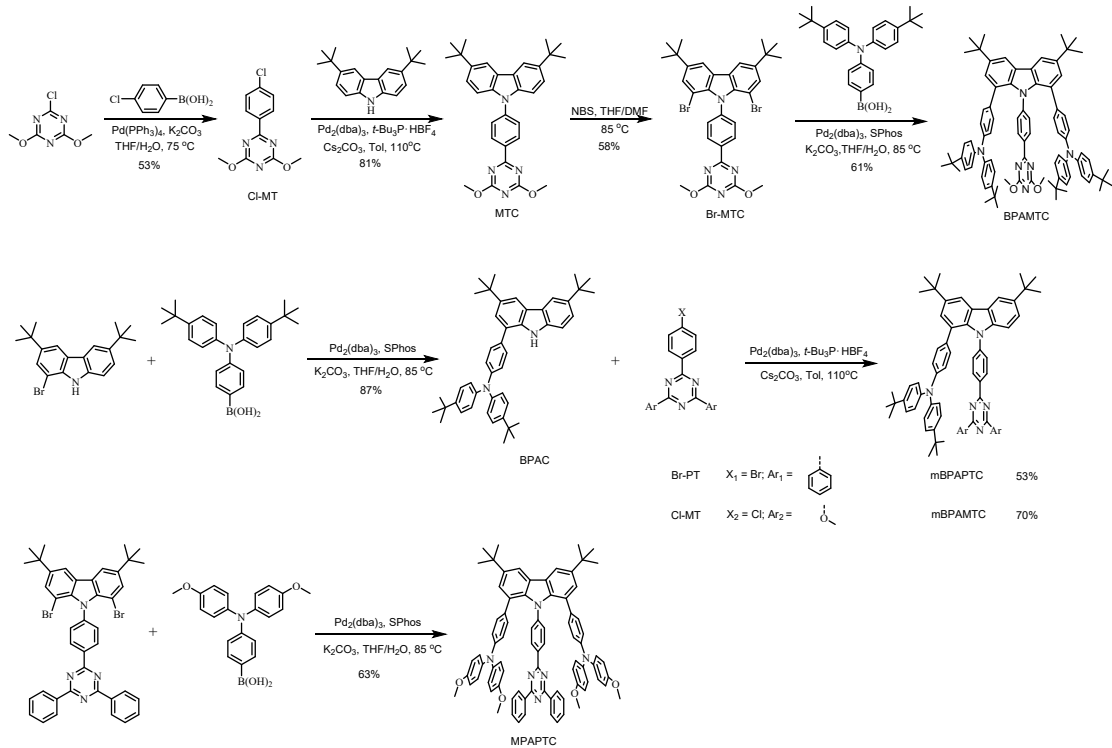
State Key Laboratory of Polymer Physics and Chemistry, Changchun Institute of Applied Chemistry, Chinese Academy of Sciences, Changchun 130022 (P. R. China).

Content

Synthesis:	2
Electrochemical properties	5
Thermal properties	5
Theoretical calculations	6
Photophysical properties	7
RMSD calculations	10
EL characteristics.....	10
NMR spectra.....	20
References.....	28

Synthesis:

All chemicals and reagents were used as received from commercial sources without further purification. Solvents for chemical synthesis were purified according to the standard procedures. 2-(4-Bromophenyl)-4,6-diphenyl-1,3,5-triazine,^[1] (4-(bis(4-methoxyphenyl)amino)phenyl)boronic acid,^[2] 2-chloro-4,6-dimethoxy-1,3,5-triazine,^[3] 1-bromo-3,6-di-tert-butyl-9H-carbazole^[4] were prepared according to references. 1,8-Dibromo-3,6-di(tert-butyl)-9-(4-(4,6-diphenyl-1,3,5-triazin-2-yl)phenyl)carbazole was synthesized according to our previous work.^[5] 4-(Bis(4-(tert-butyl)phenyl)amino)phenylboronic acid was purchased from Soochiral Chemical Science & Technology Co., Ltd in Suzhou.



Scheme S1 Synthetic routes of MPAPTC, BPAMTC, mBPAPTC and mBPAMTC.

MPAPTC: 3,6-di(*tert*-butyl)-1,8-di(4-(bis(4-methoxyphenyl)amino)phenyl)-9-(4-(4,6-diphenyl-1,3,5-triazin-2-yl)phenyl) carbazole

A mixture of 1,8-dibromo-3,6-di(*tert*-butyl)-9-(4-(4,6-diphenyl-1,3,5-triazin-2-yl)phenyl)carbazole (0.74 g, 1.0 mmol), (4-(bis(4-methoxyphenyl)amino)phenyl)boronic acid (1.1 g, 3.0 mmol), tris(dibenzylideneacetone)dipalladium (0.018 g, 0.020 mmol), 2-dicyclohexylphosphino-2',6'-dimethoxybiphenyl (0.033 g, 0.080 mmol) and K₃PO₄ (1.1 g, 4.0 mmol) were dissolved in a mixture of THF (10 mL) and water (2 mL) under an argon atmosphere. The mixture was heated to 80 °C and stirred for 24 h. After cooled to room temperature, the mixture was diluted with DCM, washed with water and brine, and dried over anhydrous Na₂SO₄. The solution was filtered and then concentrated in vacuo. The crude product was purified by column chromatography (silica, PE: DCM = 4:1) to get yellow solid. Yield: 0.75 g, 63%. ¹H NMR (500 MHz, THF-*d*₈) δ 8.93 (dt, *J* = 7.0, 1.5 Hz, 4H), 8.37 (d, *J* = 8.5 Hz, 2H), 8.26 (d, *J* = 2.0 Hz, 2H), 7.71 – 7.66 (m, 2H), 7.64 (t, *J* = 7.2 Hz, 4H), 7.28 (d, *J* = 2.0 Hz, 2H), 6.90 (d, *J* = 8.5 Hz, 2H), 6.71 (d, *J* = 8.9 Hz, 8H), 6.67 (d, *J* = 8.5 Hz, 4H), 6.45 (d, *J* = 8.9 Hz, 8H), 6.31 (d, *J* = 8.5 Hz, 4H), 3.39 (s, 12H), 1.48 (s, 18H). ¹³C NMR (126 MHz, THF-*d*₈) δ 171.82, 171.57, 156.19, 146.94, 144.76, 142.17, 140.16, 137.20, 136.21, 133.09, 132.73, 130.98, 130.00, 129.60, 129.19, 128.70, 127.74, 127.10, 126.98, 126.55, 124.76, 116.75, 114.59, 114.22, 54.26, 34.26, 31.37. MALDI-TOF (m/z) calcd

for $C_{81}H_{72}N_6O_4$ [M]⁺ : 1192.5615; Found: 1192.5590. Anal. calcd for $C_{81}H_{72}N_6O_4$ (%) : C, 81.52; H, 6.08; N, 7.04; O, 5.36. Found: C, 81.44; H, 6.13; N, 6.96.

Cl-MT: 2-(4-chlorophenyl)-4,6-dimethoxy-1,3,5-triazine

2-Chloro-4,6-dimethoxy-1,3,5-triazine (1.4 g, 8.0 mmol), (4-chlorophenyl)boronic acid (1.4 g, 8.8 mmol), tetrakis(triphenylphosphine)palladium (0.28 g, 0.24 mmol) and potassium carbonate (2.2 g, 16 mmol) were deposited in a round-bottom flask. 40 mL THF and 8 mL H₂O were added after vacuumed and nitrogen aerated for three times. The mixture was heated to 80 °C and stirred for 24 h. The reaction was cooled down to room temperature and then diluted with DCM, washed with water and brine, and dried over anhydrous Na₂SO₄. The organic phase was filtered and concentrated under reduced pressure. The crude product was purified by column chromatography to get white solid. Yield: 1.06 g, 53%. ¹H NMR (500 MHz, Chloroform-d) δ 8.44 (d, J = 8.6 Hz, 2H), 7.46 (d, J = 8.6 Hz, 2H), 4.13 (s, 6H). ¹³C NMR (126 MHz, Chloroform-d) δ 173.95, 172.90, 139.16, 133.51, 130.34, 128.81, 55.30. MALDI-TOF (m/z) calcd for $C_{11}H_{10}N_3O_2Cl$ [M]⁺ : 251.0462; Found: 251.0469.

MTC: 3,6-di-*tert*-butyl-9-(4-(4,6-dimethoxy-1,3,5-triazin-2-yl)phenyl)-9*H*-carbazole

A mixture of 3,6-di(*tert*-butyl)carbazole (0.92 g, 3.3 mmol), 2-(4-chlorophenyl)-4,6-dimethoxy-1,3,5-triazine (0.76 g, 3.0 mmol), tris(dibenzylideneacetone)dipalladium (0.055 g, 0.060 mmol), tri(*tert*-butyl)phosphine tetrafluoroborate (0.070 g, 0.24 mmol) and cesium carbonate (2.0 g, 6.0 mmol) were vacuumed and nitrogen aerated for three times. Then 25 mL degassed toluene was added and the temperature was set to 120 °C. The system was cooled down to room temperature after 24 h, diluted with DCM, washed with water and brine, and dried over anhydrous Na₂SO₄. The organic phase was filtered and concentrated under reduced pressure. The crude product was purified by column chromatography to get white solid. Yield: 1.20 g, 81%. ¹H NMR (500 MHz, Chloroform-d) δ 8.72 (d, J = 8.6 Hz, 2H), 8.14 (dd, J = 1.8, 0.9 Hz, 2H), 7.72 (d, J = 8.6 Hz, 2H), 7.53 – 7.42 (m, 4H), 4.17 (s, 6H), 1.47 (s, 18H). ¹³C NMR (126 MHz, Chloroform-d) δ 174.16, 172.94, 143.48, 142.49, 138.61, 132.98, 130.63, 125.94, 123.81 (d, J = 2.8 Hz), 116.35, 109.36, 55.31, 34.76, 31.98. MALDI-TOF (m/z) calcd for $C_{31}H_{34}N_4O_2$ [M]⁺ : 494.2682, Found: 494.2696.

Br-MTC: 1,8-dibromo-3,6-di-*tert*-butyl-9-(4-(4,6-dimethoxy-1,3,5-triazin-2-yl)phenyl)-9*H*-carbazole

MTC (0.49 g, 1.0 mmol), NBS (0.48 g, 2.7 mmol), DMF (5 mL) and THF (5 mL) were added into a 50 mL flask. The mixture was stirred at 80 °C in the dark for 12 h. After cooled to room temperature, the mixture was poured into 100 mL water, and extracted with DCM three times. The organic layer was washed with water and brine, and dried over anhydrous Na₂SO₄. The solution was filtered and concentrated in vacuo. The crude product was purified by column chromatography to give white solid. Yield: 0.39 g, 60%. ¹H NMR (500 MHz, Chloroform-d) δ 8.60 (d, J = 8.5 Hz, 2H), 8.05 (d, J = 1.7 Hz, 2H), 7.64 – 7.55 (m, 4H), 4.17 (s, 6H), 1.44 (s, 18H). ¹³C NMR (126 MHz, Chloroform-d) δ 174.34, 172.99, 144.96, 142.70, 136.93, 135.85, 132.82, 130.16, 128.56, 125.63, 115.46, 103.79, 55.34, 34.68, 31.76. MALDI-TOF (m/z) calcd for $C_{31}H_{32}N_4O_2Br_2$ [M]⁺ : 650.0892, Found: 650.0914.

BPAMTC: 3,6-di(*tert*-butyl)-1,8-di(4-(bis(4-(*tert*-butyl)phenyl)amino)phenyl)-9-(4-(4,6-dimethoxy-1,3,5-triazin-2-yl)phenyl) carbazole

BPAMTC was prepared from Br-MTC (0.39 g, 0.60 mmol) and 4-(bis(4-(*tert*-butyl)phenyl)amino)phenylboronic acid (0.60 g, 1.5 mmol) by the same procedure of MPAPTC. Yellow-green solid. Yield: 0.58 g, 81%. ¹H NMR (500 MHz, Chloroform-d) δ 8.17 (s, 2H), 8.06 – 8.02 (m, 2H), 7.28 (d, J = 2.0 Hz, 2H), 7.13 (d, J = 8.2 Hz, 8H), 6.92 – 6.76 (m, 10H), 6.72 (d, J = 8.0 Hz, 4H), 6.55 (s, 4H), 4.06 (s, 6H), 1.49 (s, 18H), 1.29 (s, 36H). ¹³C NMR (126 MHz, Chloroform-d) δ 174.11, 172.67, 145.44, 144.50, 142.53, 137.31, 132.09, 129.58, 127.74, 127.35, 126.24, 125.58, 124.46, 124.18, 119.76, 114.56, 54.93, 34.44, 33.98, 31.77, 31.18. MALDI-TOF (m/z) calcd for

$C_{83}H_{92}N_6O_2$ [M]⁺ : 1204.7282, Found: 1204.7329. Anal. calcd for $C_{83}H_{92}N_6O_2$ (%) : C, 82.68; H, 7.69; N, 6.97; O, 2.65. Found: C, 82.51; H, 7.56; N, 6.84.

BPAC: 4-(*tert*-butyl)-*N*-(4-(*tert*-butyl)phenyl)-*N*-(4-(3,6-di-*tert*-butyl-9*H*-carbazol-1-yl)phenyl)aniline
1-Bromo-3,6-di-*tert*-butyl-9*H*-carbazole (1.4 g, 4.0 mmol), 4-(bis(4-(*tert*-butyl)phenyl)amino)phenyl-boronic acid (1.7 g, 4.2 mmol), tris(dibenzylideneacetone)dipalladium (0.073 g, 0.080 mmol), 2-dicyclohexylphosphino-2',6'-dimethoxybiphenyl (0.13 g, 0.32 mmol) and K_3PO_4 (1.1 g, 8.0 mmol) were deposited in a round-bottom flask. 40 mL THF and 8 mL H_2O were added after vacuumed and nitrogen aerated for three times. The mixture was heated to 80 °C and stirred for 24 h. The reaction was cooled down to room temperature and then diluted with DCM, washed with water and brine, and dried over anhydrous Na_2SO_4 . The organic phase was filtered and concentrated under reduced pressure. The crude product was purified by column chromatography to get white solid. Yield: 2.21 g, 87%. ¹H NMR (400 MHz, Benzene-*d*₆) δ 8.34 (d, *J* = 1.9 Hz, 1H), 8.30 (d, *J* = 1.8 Hz, 1H), 7.67 (d, *J* = 1.8 Hz, 1H), 7.62 (s, 1H), 7.52 – 7.43 (m, 3H), 7.35 – 7.24 (m, 10H), 6.99 (dd, *J* = 8.5, 0.6 Hz, 1H), 1.46 (s, 9H), 1.44 (s, 9H), 1.25 (s, 18H). ¹³C NMR (101 MHz, Benzene-*d*₆) δ 148.13, 146.24, 145.92, 143.01, 142.38, 138.73, 136.66, 133.74, 129.63, 126.73, 124.98, 124.89, 124.64, 124.34, 124.05, 123.97, 123.87, 116.70, 115.60, 110.84, 34.91, 34.84, 34.40, 32.25, 31.58, 27.26. MALDI-TOF (m/z) calcd for $C_{46}H_{54}N_2$ [M]⁺ : 634.4287; Found: 634.4306.

mBPAPTC: 3,6-di(*tert*-butyl)-1-(4-(bis(4-(*tert*-butyl)phenyl)amino)phenyl)-9-(4-(4,6-diphenyl-1,3,5-triazin-2-yl)phenyl) carbazole

A mixture of BPAC (0.70 g, 1.1 mmol), 2-(4-bromophenyl)-4,6-diphenyl-1,3,5-triazine (0.39 g, 1.0 mmol), tris(dibenzylideneacetone)dipalladium (0.018 g, 0.020 mmol), 2-dicyclohexylphosphino-2',6'-dimethoxy- biphenyl (0.033 g, 0.080 mmol) and sodium *tert*-butoxide (0.19 g, 2.0 mmol) were vacuumed and nitrogen aerated for three times. Then 10 mL degassed toluene was added and the temperature was set to 120 °C. The system was cooled down to room temperature after 24 h, diluted with DCM, washed with water and brine, and dried over anhydrous Na_2SO_4 . The organic phase was filtered and concentrated under reduced pressure. The crude product was purified by column chromatography to get green solid. The product was then further purified with toluene / ethyl alcohol. Yield: 0.50 g, 53%. ¹H NMR (500 MHz, THF-*d*₈) δ 8.92 – 8.83 (m, 4H), 8.77 (d, *J* = 8.5 Hz, 2H), 8.25 (dd, *J* = 8.6, 1.9 Hz, 2H), 7.70 – 7.56 (m, 6H), 7.47 (dd, *J* = 8.7, 1.9 Hz, 1H), 7.42 (d, *J* = 1.9 Hz, 1H), 7.35 (dd, *J* = 8.6, 4.7 Hz, 3H), 6.97 (d, *J* = 8.5 Hz, 2H), 6.94 (d, *J* = 8.6 Hz, 4H), 6.71 (d, *J* = 8.6 Hz, 4H), 6.58 (d, *J* = 8.5 Hz, 2H), 1.51 (s, 1H), 1.47 (s, 9H), 1.06 (s, 18H). ¹³C NMR (126 MHz, THF-*d*₈) δ 172.53, 172.01, 147.37, 146.38, 145.56, 144.33, 143.95, 143.83, 141.29, 137.07, 137.02, 134.49, 133.40, 133.05, 130.36, 129.85, 129.78, 129.39, 128.41, 126.97, 126.89, 126.46, 126.36, 125.42, 124.64, 124.42, 120.67, 116.75, 115.81, 110.14, 35.19, 34.49, 32.19, 32.16, 31.44. MALDI-TOF (m/z) calcd for $C_{67}H_{67}N_5$ [M]⁺ : 941.5396; Found: 941.5356. Anal. calcd for $C_{67}H_{67}N_5$ (%) : C, 85.40; H, 7.17; N, 7.43. Found: C, 85.24; H, 7.21; N, 7.35.

mBPAMTC: 3,6-di(*tert*-butyl)-1-4-(bis(4-(*tert*-butyl)phenyl)amino)phenyl)-9-(4-(4,6-dimethoxy-1,3,5-triazin-2-yl)phenyl) carbazole

A mixture of BPAC (0.89 g, 1.4 mmol), MTCI (0.30 g, 1.2 mmol), tris(dibenzylideneacetone)dipalladium (0.022 g, 0.024 mmol), tri(*tert*-butyl)phosphine tetrafluoroborate (0.028 g, 0.096 mmol) and cesium carbonate (0.78 g, 2.4 mmol) were vacuumed and nitrogen aerated for three times. Then 25 mL degassed toluene was added and the temperature was set to 120 °C. The system was cooled down to room temperature after 24 h, diluted with DCM, washed with water and brine, and dried over anhydrous Na_2SO_4 . The organic phase was filtered and concentrated under reduced pressure. The crude product was purified by column chromatography to get yellow-green solid. Yield: 0.71 g, 70%. ¹H NMR (500 MHz, Chloroform-*d*) δ 8.42 (d, *J* = 8.6 Hz, 2H), 8.21 – 8.06 (m, 2H),

7.48 – 7.37 (m, 2H), 7.32 (d, J = 8.7 Hz, 1H), 7.22 (d, J = 8.5 Hz, 2H), 7.04 (d, J = 55.6 Hz, 6H), 6.80 (s, 6H), 4.14 (s, 6H), 1.51 (s, 9H), 1.47 (s, 9H), 1.29 (s, 18H). ^{13}C NMR (126 MHz, Chloroform-*d*) δ 174.25, 172.94, 145.18, 143.61, 143.52, 140.32, 136.13, 132.34, 129.20, 127.24, 125.72, 123.85, 123.77, 121.59, 116.11, 115.08, 109.53, 55.26, 34.77, 34.74, 34.17, 32.02, 31.98, 31.42. $\text{C}_{57}\text{H}_{63}\text{N}_5\text{O}_2$ [M]⁺: 849.4982; Found: 849.5005. Anal. calcd for $\text{C}_{57}\text{H}_{63}\text{N}_5\text{O}_2$ (%): C, 80.53; H, 7.47; N, 8.24; O, 3.76. Found: C, 80.36; H, 7.33; N, 7.38.

Electrochemical properties

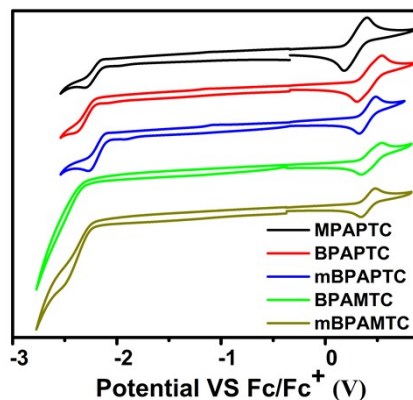


Fig. S1. Cyclic voltammogram of MPAPTC, BPAPTC, mBPAPTC, BPAMTC and mBPAMTC.

Thermal properties

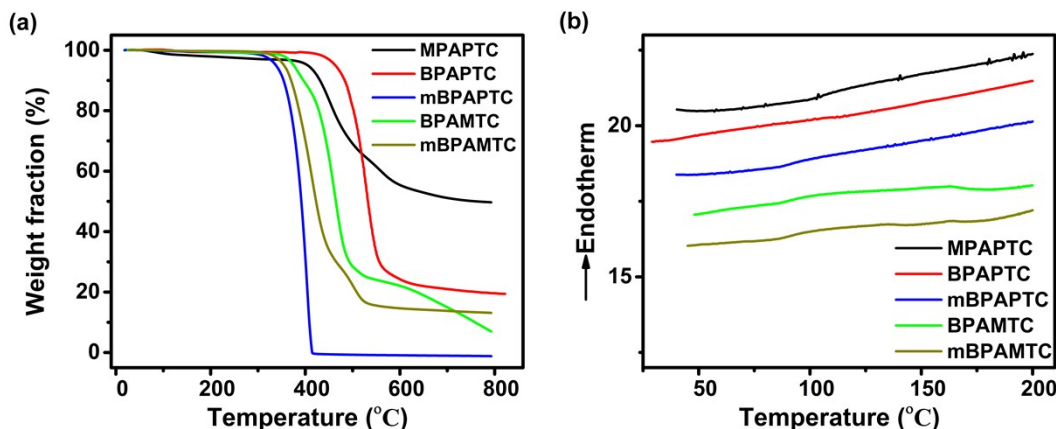


Fig. S2. a) TGA traces of BPAPTC, mBPAPTC, BPAMTC, mBPAMTC and MPAPTC recorded at a heating rate of 10 °C min⁻¹. b) DSC traces of BPAPTC, mBPAPTC, BPAMTC, mBPAMTC and MPAPTC recorded at a heating rate of 10 °C min⁻¹.

Table S1. Thermal stability properties of BAPTC, mBPAPTC, BPAMTC, mBPAMTC and MPAPTC.

Compound	T_d (°C)	T_g (°C)
BPAPTC	462	--
mBPAPTC	326	93
BPAMTC	376	93
mBPAMTC	355	94
MPAPTC	405	111

Theoretical calculations

Table S2. Computed transition energies (E_{VA}), oscillator strengths (f_{VA}) and configuration interaction description of S_1 , T_1 , T_2 and T_3 transitions using TD-BMK and 6-31G(d) basis set in toluene on the basis of S_0 geometries.

S ₀ geometry in toluene						
	functional		E _{VA} (eV)	CI description	C _j %	f _{VA}
MPAPTC	BMK	S ₁	2.9291	HOMO→LUMO	89.13	0.0009
				HOMO-1→LUMO	9.39	
		T ₁	2.9097	HOMO-1→LUMO	83.83	0.0000
		T ₂	3.0092	HOMO→LUMO	74.85	0.0000
BPAPTC	BMK	T ₃	3.0498	HOMO→LUMO+1	86.05	0.0000
		S ₁	2.9952	HOMO→LUMO	88.6	0.0024
		T ₁	2.9666	HOMO→LUMO	78.3	0.0000
		T ₂	3.0660	HOMO-2→LUMO	37.0	0.0000
mBPAPTC	BMK	T ₃	3.0877	HOMO-1→LUMO	81.9	0.0000
		S ₁	3.1971	HOMO→LUMO	97.31	0.0126
		T ₁	3.0783	HOMO-1→LUMO	37.29	0.0000
		T ₂	3.1691	HOMO→LUMO+2	30.40	0.0000
BPAMTC	BMK	T ₃	3.1978	HOMO→LUMO	82.98	0.0000
		S ₁	3.2582	HOMO→LUMO	97.05	0.0076
		T ₁	3.1757	HOMO-2→LUMO	48.57	0.0000
		T ₂	3.1812	HOMO-3→LUMO+1	21.16	0.0000
mBPAMTC	BMK	T ₃	3.2411	HOMO→LUMO	91.37	0.0000
		S ₁	3.3424	HOMO→LUMO	96.90	0.0160
		T ₁	3.1624	HOMO→LUMO+1	31.13	0.0000
				HOMO-2→LUMO+3	21.85	
MPAPTC		T ₂	3.2216	HOMO-1→LUMO	40.00	0.0000
		T ₃	3.3348	HOMO→LUMO	83.10	0.0000

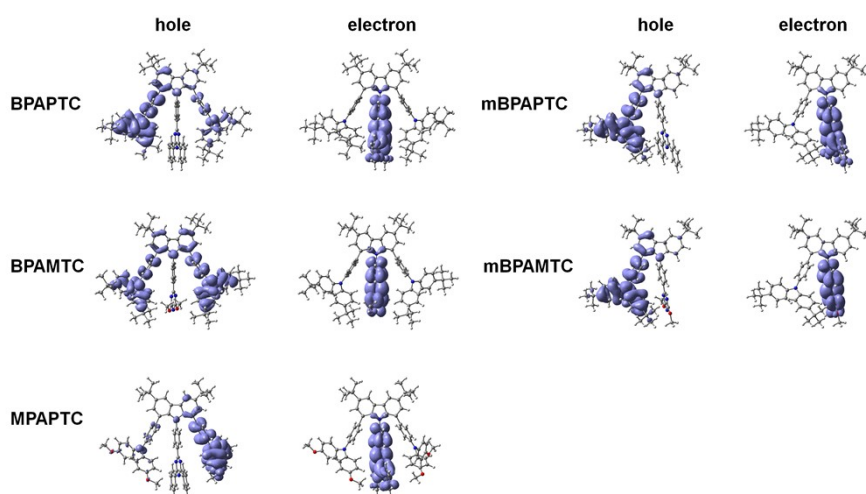


Fig. S3. NTOs of the S₁ states for BPAPTC, mBPAPTC, BPAMTC, mBPAMTC and MPAPTC.

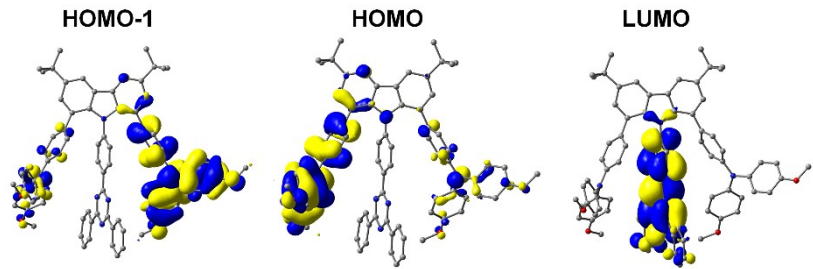


Fig. S4. Distributions of HOMO-1, HOMO and LUMO of MPAPTC.

Photophysical properties

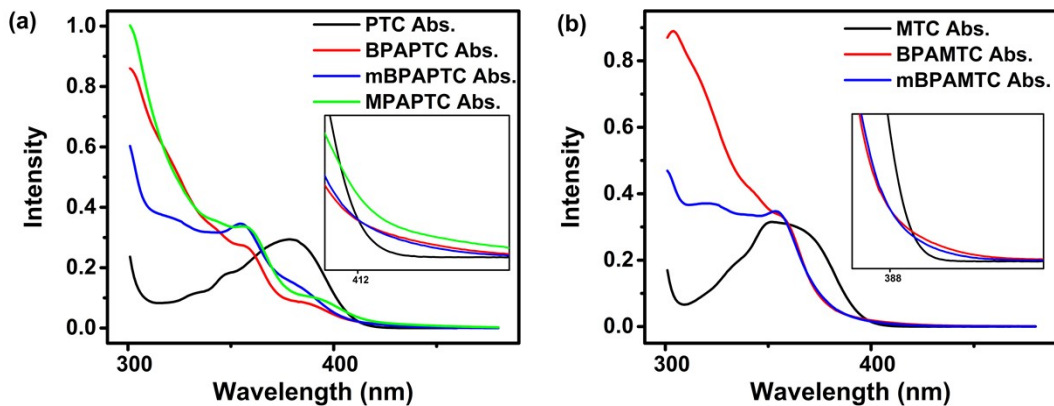


Fig. S5. The UV-vis absorption spectra of (a) PTC, BPAPTC, mBPAPTC and MPAPTC; (b) MTC, BPAMTC and mBPAMTC measured in toluene with concentration of 10^{-5} M. Inset: UV-vis absorption spectra zoomed at around 412 nm and 388 nm, respectively.

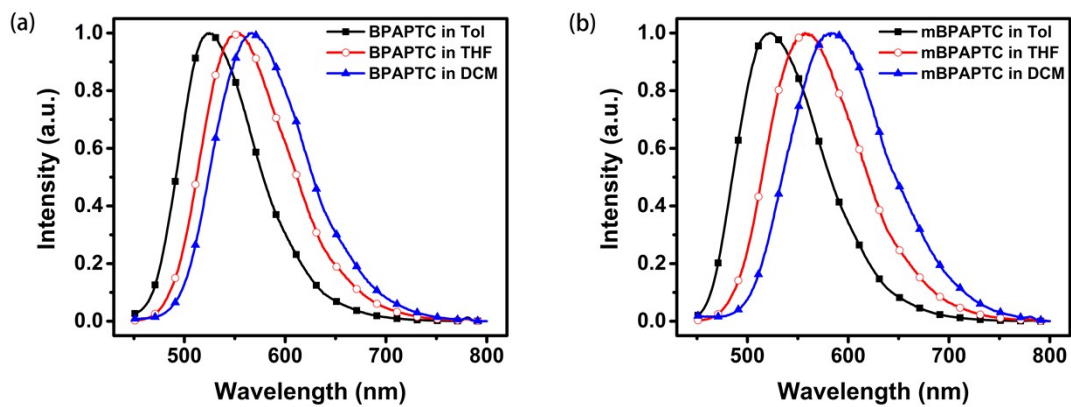


Fig. S6. The PL spectra of (a) BPAPTC and (b) measured in different solvents with concentration of 10^{-5} M.

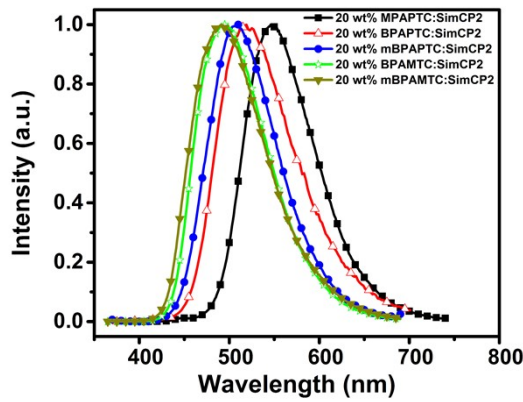


Fig. S7. The PL spectra of the five compounds measured in 20 wt% doped film with SimCP2 as the host.

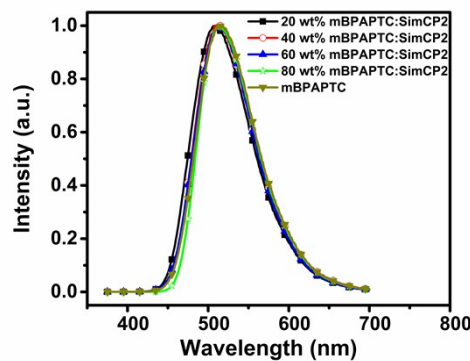


Fig. S8. PL spectra of mBPAPTC doped in SimCP2 with different ratios.

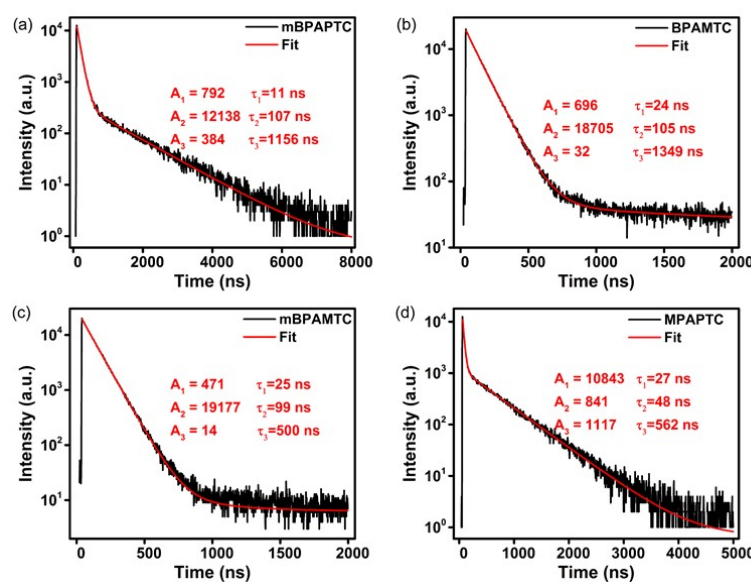


Fig. S9. Transient decay spectra and exponential fitting curves of five molecules in toluene.

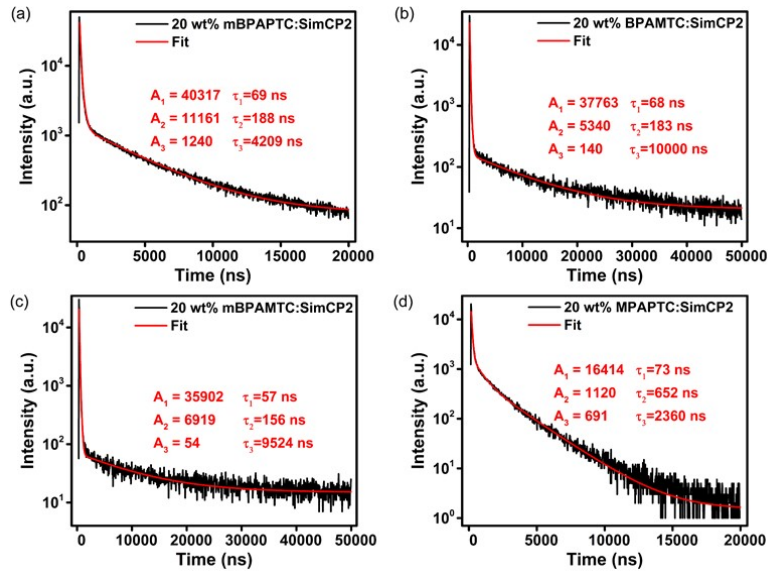


Fig. S10. Transient decay spectra and exponential fitting curves of the five compounds in doped film at 300 K.

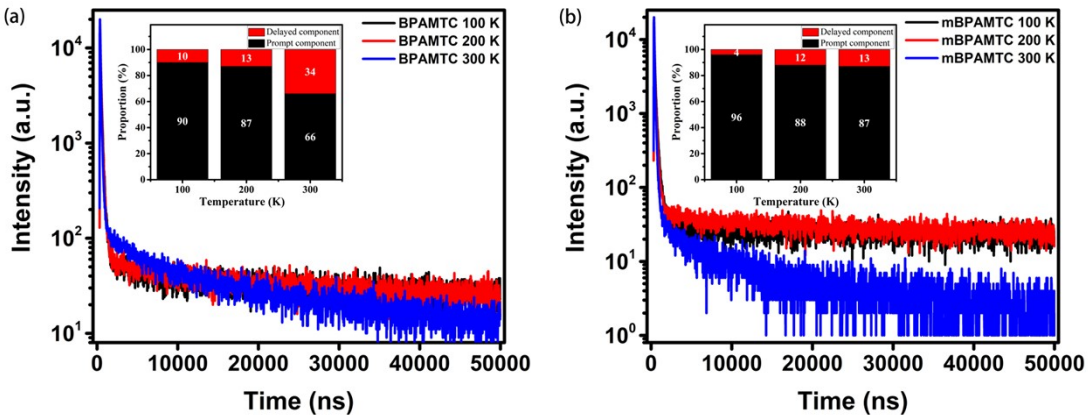


Fig. S11. Temperature dependent PL transient decay spectra of (a) 20 wt% BPAMTC: SimCP2 film and (b) 20 wt% mBPAMTC: SimCP2 film.

Table S3. The rate constants of photophysical process of BAPTC, mBPAPTC, BPAMTC, mBPAMTC and MPAPTC.

compound	K_{PF} (10^6 s^{-1})	K_{DF} (10^5 s^{-1})	K_{ISC} (10^6 s^{-1})	K_{RISC} (10^5 s^{-1})	K_r (10^5 s^{-1})	K_{nr} (10^5 s^{-1})
BAPTC	2.05	1.59	1.66	8.43	4.65	0.52
mBPAPTC	3.48	2.16	2.55	8.11	9.78	1.09
BPAMTC	4.85	0.50	2.31	0.96	16.2	6.05
mBPAMTC	6.84	0.94	2.97	1.67	27.0	12.1
MPAPTC	2.05	1.58	1.35	4.64	3.53	4.49

RMSD calculations

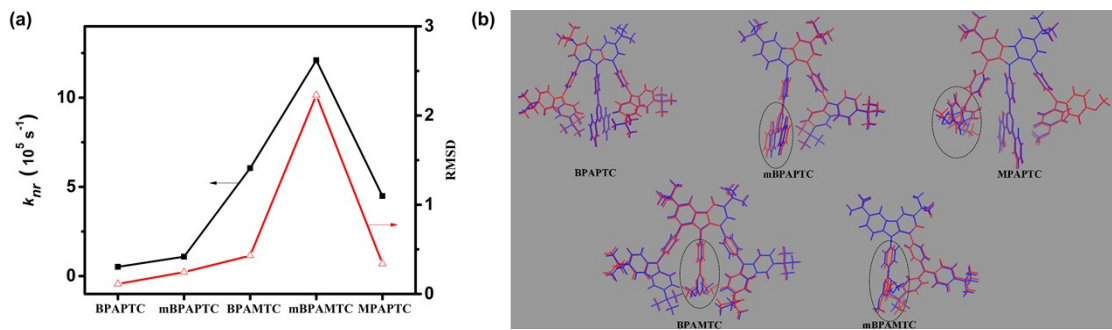


Fig. S12. (a) The plots of K_{nr} s and RMSDs of the five compounds; (b)The optimized ground state (blue) and excited state (red) configuration of the studied molecules.

Table S4. The RMSD values of BAPTC, mBPAPTC, BPAMTC, mBPAMTC and MPAPTC.

	BAPTC	mBPAPTC	BPAMTC	mBPAMTC	MPAPTC
RMSD	0.1117	0.2447	0.4296	2.2288	0.3384

EL characteristics

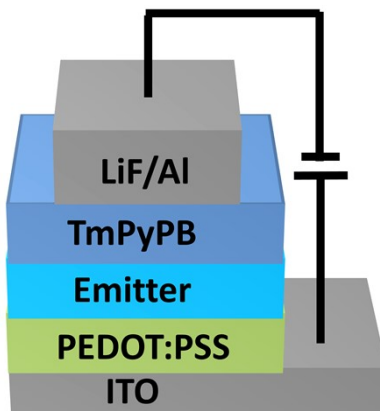


Fig. S13. Device structure.

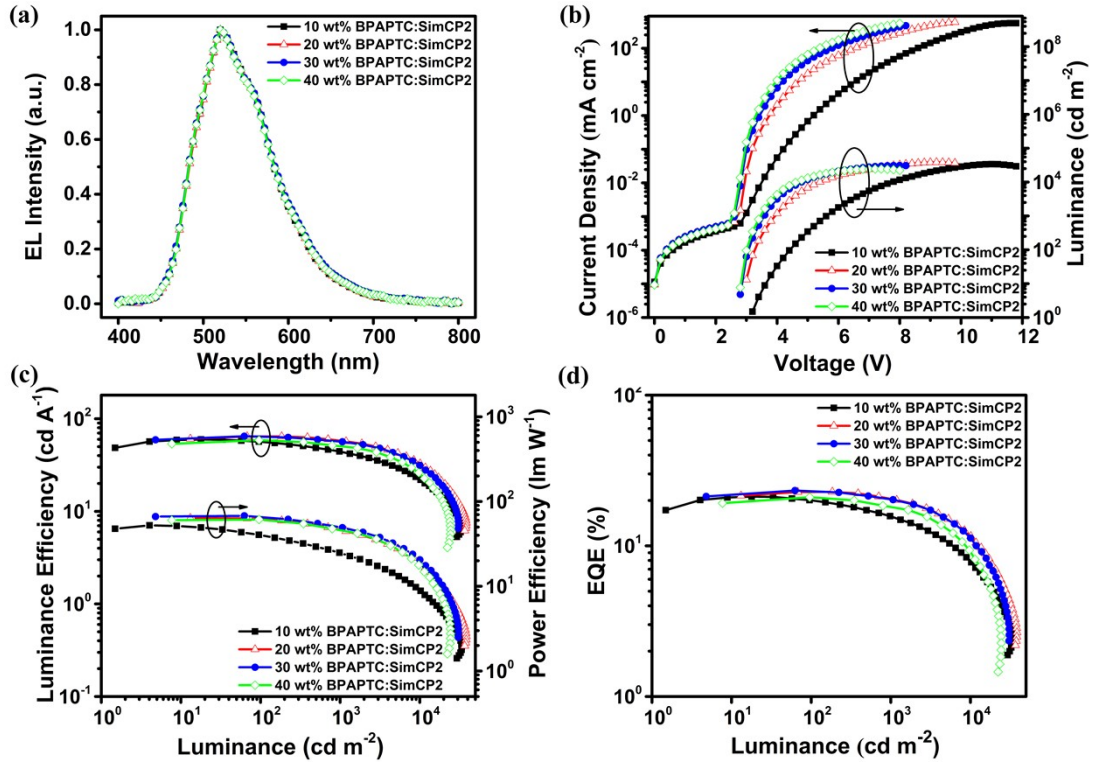


Fig. S14. EL performance of BPAPTC with different doped ratios; (a) EL spectra; (b) Current density-voltage-luminance curves; (c) Luminous efficiency-luminance-power efficiency curves; (d) EQE-luminance curves.

Table S5. EL performances of BPAPTC with different doped ratios.

Device	Max performance						Device performance at 1000/5000/10000 cd m ⁻²			
	EL [nm]	V _{on} [V]	L	LE	PE	EQE [%]	V _d [V]	LE [cd A ⁻¹]	PE [lm W ⁻¹]	EQE [%]
			[cd m ⁻²] A ⁻¹	[cd A ⁻¹]	[lm W ⁻¹]					
10 wt%	520	3.1	33804	59.7	52.3	21.2	5.6/6.9/7.8	44.6/30.4/22.3	25.0/13.6/ 9.3	15.6/10.6/ 7.9
20 wt%	520	2.8	38481	64.5	63.6	22.8	3.9/4.7/5.4	58.1/43.6/32.7	46.0/28.3/ 19.4	20.4/15.3/ 11.6
30 wt%	520	2.7	30808	64.8	67.8	23.3	3.6/4.3/4.8	56.6/41.5/31.1	50.3/30.9/ 20.5	20.4/15.0/ 11.2
40 wt%	520	2.7	24520	58.7	61.4	21.0	3.5/4.1/4.6	50.4/35.8/25.4	45.7/28.0/ 17.1	18.1/13.0/ 9.1

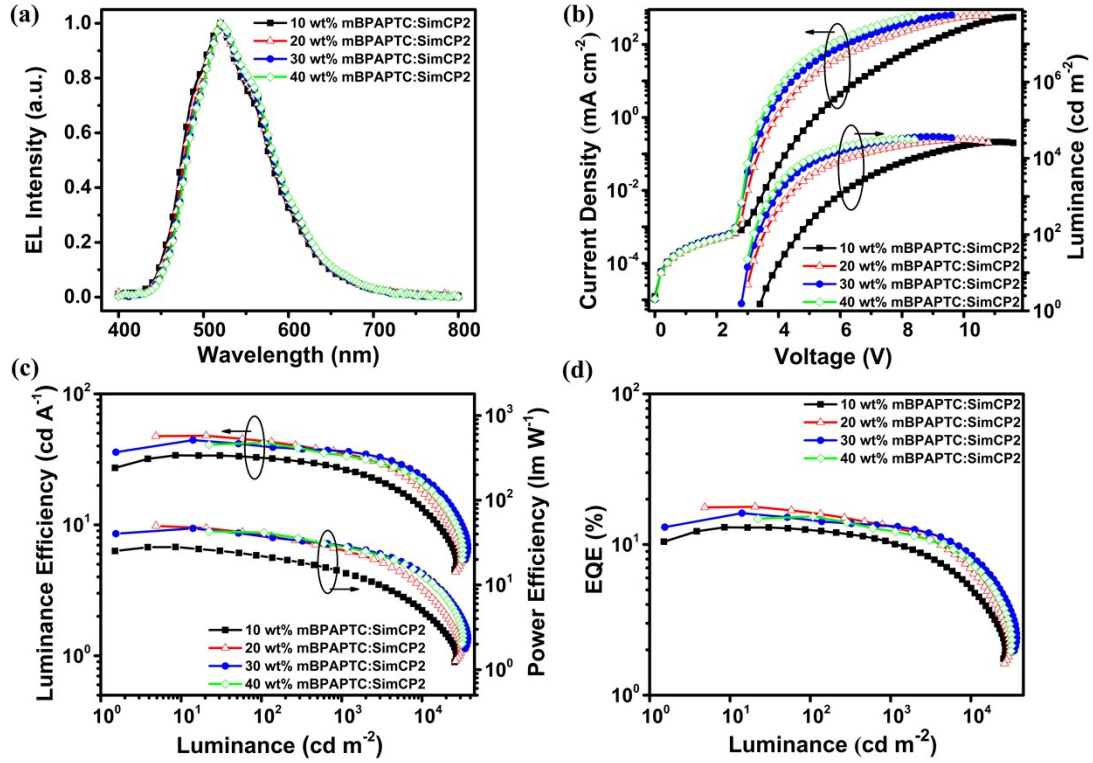


Fig. S15. EL performance of mBPAPTC with different doped ratios; (a) EL spectra; (b) Current density-voltage-luminance curves; (c) Luminous efficiency-luminance-power efficiency curves; (d) EQE-luminance curves.

Table S6. EL performances of mBPAPTC with different doped ratios.

Device	Max performance						Device performance at 1000/5000/10000 cd m ⁻²			
	EL [nm]	V _{on} [V]	L [cd m ⁻²]	LE [cd A ⁻¹]	PE [lm W ⁻¹]	EQE [%]	V _d [V]	LE [cd A ⁻¹]	PE [lm W ⁻¹]	EQE [%]
10 wt%	520	3.3	26935	33.9	28.0	13.0	5.9/7.4/8.5	27.1/18.5/13.4	14.3/7.8/ 5.0	10.3/7.1/ 5.1
20 wt%	520	2.9	30590	47.9	50.0	17.8	4.3/5.4/6.3	35.5/25.0/18.3	25.9/14.6/ 9.1	13.2/9.4/ 6.7
30 wt%	520	2.8	37160	44.4	46.5	16.1	3.9/4.7/5.4	36.6/29.6/23.3	29.1/19.6/ 13.8	13.3/10.7/ 8.5
40 wt%	520	2.8	32433	42.3	42.9	15.3	3.7/4.5/5.0	33.9/26.9/21.1	28.3/18.7/ 13.0	12.3/9.7/ 7.6

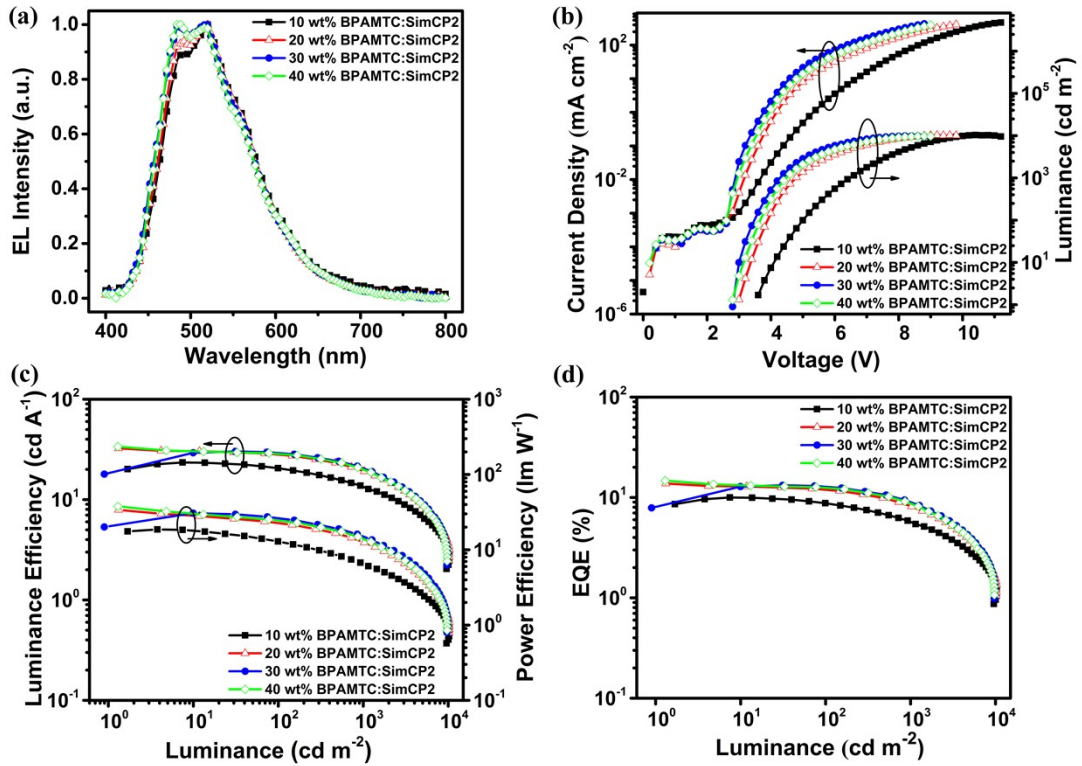


Fig. S16. EL performance of BPAMTC with different doped ratios; (a) EL spectra; (b) Current density-voltage-luminance curves; (c) Luminous efficiency-luminance-power efficiency curves; (d) EQE-luminance curves.

Table S7. EL performances of BPAMTC with different doped ratios.

Device	Max performance						Device performance at 1000/5000/10000 cd m ⁻²			
	EL [nm]	V _{on} [V]	L [cd m ⁻²]	LE [cd A ⁻¹]	PE [lm W ⁻¹]	EQE [%]	V _d [V]	LE [cd A ⁻¹]	PE [lm W ⁻¹]	EQE [%]
10 wt%	492/519	3.5	10326	23.4	18.6	10.0	6.5/8.3/10.2	13.5/6.7/3.3	6.5/2.6/1.0	5.7/3.3/1.1
20 wt%	492/519	3.0	10283	32.5	34.0	13.8	4.8/6.6/8.9	19.0/8.8/3.6	12.6/4.3/0.93	8.2/3.7/1.5
30 wt%	484/519	2.8	9848	30.2	30.6	13.2	4.3/5.7/--	20.7/9.2/--	14.9/5.0/--	9.0/4.0/--
40 wt%	486/516	2.8	9723	33.7	37.8	14.7	4.5/6.1/--	20.1/8.6/--	13.9/4.5/--	8.8/3.8/--

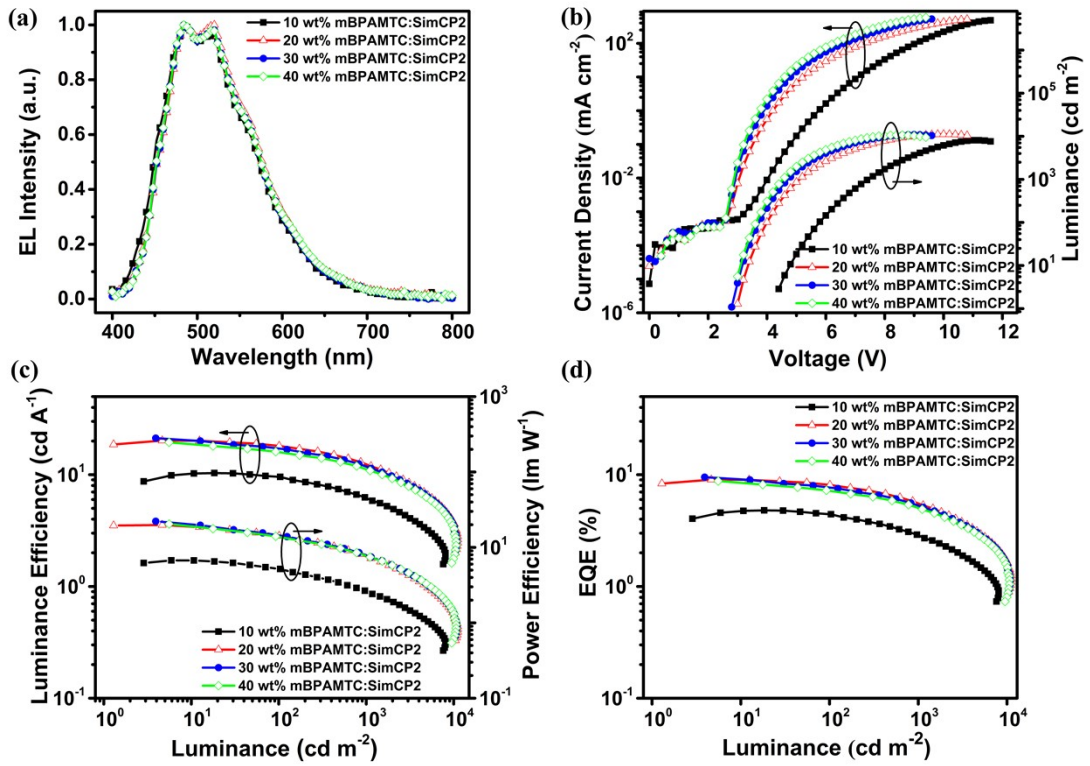


Fig. S17. EL performance of mBPAMTC with different doped ratios; (a) EL spectra; (b) Current density-voltage-luminance curves; (c) Luminous efficiency-luminance-power efficiency curves; (d) EQE-luminance curves.

Table S8. EL performances of mBPAMTC with different doped ratios.

Device	Max performance						Device performance at 1000/5000/10000 cd m ⁻²			
	EL [nm]	V _{on} [V]	L [cd m ⁻²]	LE [cd A ⁻¹]	PE [lm W ⁻¹]	EQE [%]	V _d [V]	LE [cd A ⁻¹]	PE [lm W ⁻¹]	EQE [%]
10 wt%	484/ 520	4.2	8055	10.3	6.7	4.8	7.4/9.6/--	6.2/3.2/--	2.6/1.1/ --	2.9/1.5/ --
20 wt%	484/ 520	3.0	11113	20.0	19.8	9.0	5.1/7.0/8.9	12.4/6.5/3.7	7.6/2.9/ 1.3	5.5/2.9/ 1.6
30 wt%	484/ 520	2.8	10864	21.2	22.2	9.5	4.7/6.4/8.1	11.8/6.4/3.5	7.9/3.1/ 0.69	5.3/2.9/ 1.6
40 wt%	484/ 520	2.8	10677	19.5	20.4	8.8	4.6/6.1/7.7	11.2/6.2/3.3	7.7/3.3/ 1.3	5.0/2.8/ 1.5

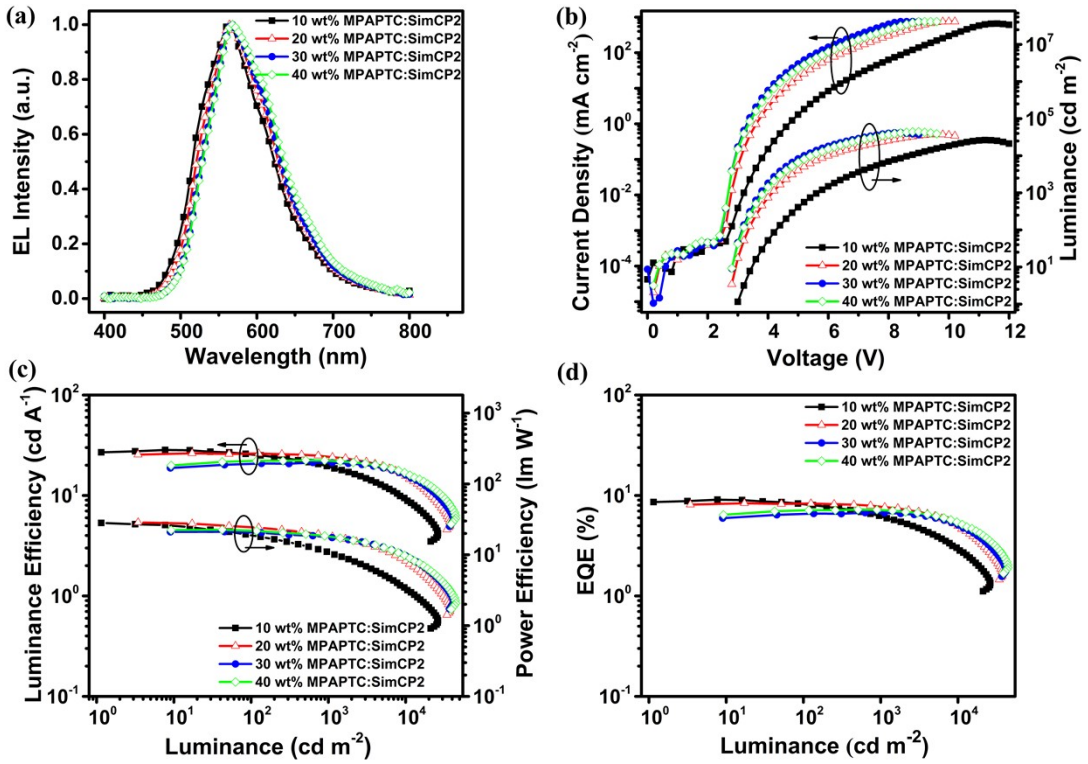


Fig. S18. EL performance of MPAPTC with different doped ratios; (a) EL spectra; (b) Current density-voltage-luminance curves; (c) Luminous efficiency-luminance-power efficiency curves; (d) EQE-luminance curves.

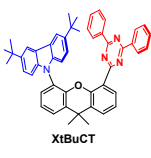
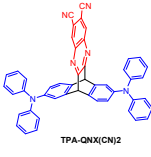
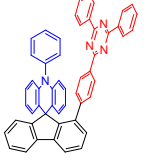
Table S9. EL performances of MPAPTC with different doped ratios.

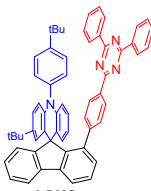
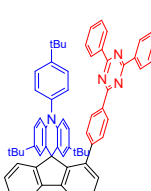
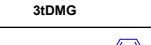
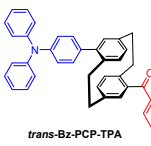
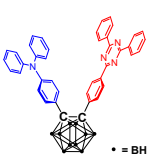
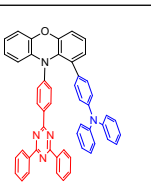
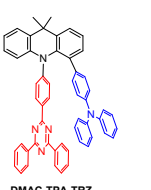
Device	Max performance						Device performance at 1000/5000/10000 cd m ⁻²			
	EL [nm]	V _{on} [V]	L [cd m ⁻²]	LE [cd A ⁻¹]	PE [lm W ⁻¹]	EQE [%]	V _d [V]	LE [cd A ⁻¹]	PE [lm W ⁻¹]	EQE [%]
10 wt%	564	3.0	26265	28.4	28.1	9.1	5.6/7.5/8.7	19.4/12.6/9.2	10.7/5.3/ 3.3	6.2/4.0/ 2.9
20 wt%	564	2.7	37611	26.3	28.6	8.4	4.1/5.2/6.0	24.4/19.7/15.7	18.5/11.8/ 8.3	7.7/6.3/ 5.0
30 wt%	568	2.7	41639	21.2	21.2	6.7	3.8/4.6/5.2	21.3/18.9/16.1	17.8/13.0/ 9.7	6.7/6.0/ 5.1
40 wt%	568	2.7	44394	22.4	22.6	7.2	3.8/4.8/5.4	22.4/19.4/16.7	18.1/12.7/ 9.7	7.2/6.3/ 5.4

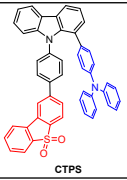
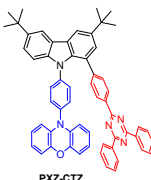
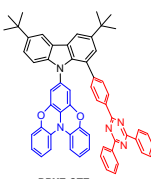
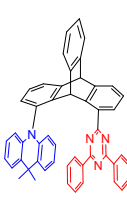
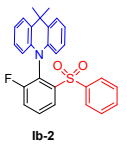
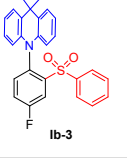
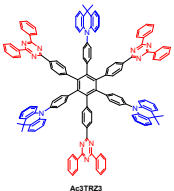
Table S10. EQE values of TSCT compounds with different doped ratios.

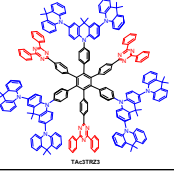
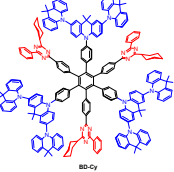
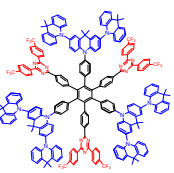
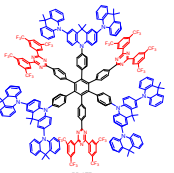
Compounds	Devices	EQE (%)			
		10 wt%	20 wt%	30 wt%	40 wt%
BPAPTC (Chem. Commun.)	1	--	24.3	--	--
	2	--	24.3	--	--
	3	--	24.2	--	--
BPAPTC (this work)	1	21.2	22.8	21.3	21.0
	2	20.8	21.1	23.3	21.0
	3	19.2	22.7	22.5	17.8
mBPAPTC	1	13.0	16.8	16.1	15.3
	2	12.2	17.8	14.5	12.4
	3	12.3	16.9	15.1	11.9
BPAMTC	1	9.7	11.0	12.9	13.0
	2	10.0	12.9	13.2	13.6
	3	9.1	13.8	12.9	14.7
mBPAMTC	1	4.8	7.8	9.0	8.8
	2	4.1	9.0	8.1	6.7
	3	3.7	8.9	9.5	7.3
MPAPTC	1	9.1	8.4	6.7	7.2
	2	8.4	7.8	6.6	6.6
	3	9.1	7.7	6.6	6.3

Table S11. Devices performances of TSCT-based TADF compounds.

Compounds	Φ_{PL} Tol/ film (%)	EL (nm)	V _{on} (V)	EQE _{max} (%)	Process	refs
	7.7/66	584	3.2	10	Vacuum- deposition	<i>J. Am. Chem. Soc.</i> 2017 , <i>139</i> , 4894-4900
	6.0/35	488	3.7	4	Vacuum- deposition	
	35 /--	573	--	9.4	Vacuum- deposition	<i>J. Am. Chem. Soc.</i> 2015 , <i>137</i> , 11908-11911
	25/--	542	--	4.0	Vacuum- deposition	
	78/96	~500	2.8	27.4	Vacuum- deposition	<i>Nat. Mater.</i> 2020 , <i>19</i> , 1332-1338
	69/92	~500	2.6	21.7	Vacuum- deposition	
	51/88	~500	3.0	18.5	Vacuum- deposition	
	12/32	~500	3.4	4.3	Vacuum- deposition	
	--/53	508	3.6	12.5	Vacuum- deposition	<i>J. Am. Chem. Soc.</i> 2020 , <i>142</i> , 17756-17765

	--/89	508	4.0	23.1	Vacuum-deposition	
	--/87	504	< 3	30.8	Vacuum-deposition	<i>Adv. Mater.</i> 2020 , 2003885
		486	6-7.5	16.2	Solution	
	--/86	518	< 3	26.3	Vacuum-deposition	
		504	6-7.5	20.1	Solution	
	45/12 (at 404, 492 nm)	--	--	--	--	<i>Chem. Commun.</i> 2018 , 54, 9278
	60/15 (at 404, 455 nm)	--	--	--	--	
	3/97	586	6.3	11.0	Vacuum-deposition	<i>Angew. Chem. Int. Ed.</i> 2016 , 55, 7171-7175
	3/55	631	4.4	10.1	Vacuum-deposition	
	--/50	~ 500	~ 2.5	10.5	Vacuum-deposition	<i>J. Phys. Chem. C</i> 2019 , 123, 12400-12410
	--/100	~ 546	~ 2.5	22	Vacuum-deposition	

	10.8/24	~ 500	2.6	2.55	Vacuum-deposition	<i>Chem. Mater.</i> 2019 , <i>31</i> , 5981-5992
	--/55	~520	<3	16.57	Vacuum-deposition	<i>Angew. Chem. Int. Ed.</i> 2021 , <i>60</i> , 3994-3998
	--/78	~529	~3.3	19.71	Vacuum-deposition	
	--/99	~515	~3.0	23.96	Vacuum-deposition	
	84/76	498	~4.0	19.2 (w/o oc sheet)	Vacuum-deposition	<i>Nat. Photon.</i> 2020 , <i>14</i> , 643-649
				29.0 (w/ oc sheet)		
	--/96.8	506	4.4	12.3	Solution	<i>Adv. Optical Mater.</i> 2021 , <i>9</i> , 2100180
	--/99.7	508	4.0	20.1	Solution	
	--/88.8	514	4.4	11.28	Solution	
	--/54	492	2.9	11.0	Solution	<i>Chem. Sci.</i> , 2019 , <i>10</i> , 2915-2923

	--/63	503	2.9	14.2	Solution	
	--/74	477	2.9	18.2	Solution	<i>Angew. Chem. Int. Ed.</i> 2021 , <i>60</i> , 16585-16593
	--/86	552	2.8	21.9	Solution	
	--/49	626	3.0	10.3	Solution	

NMR spectra

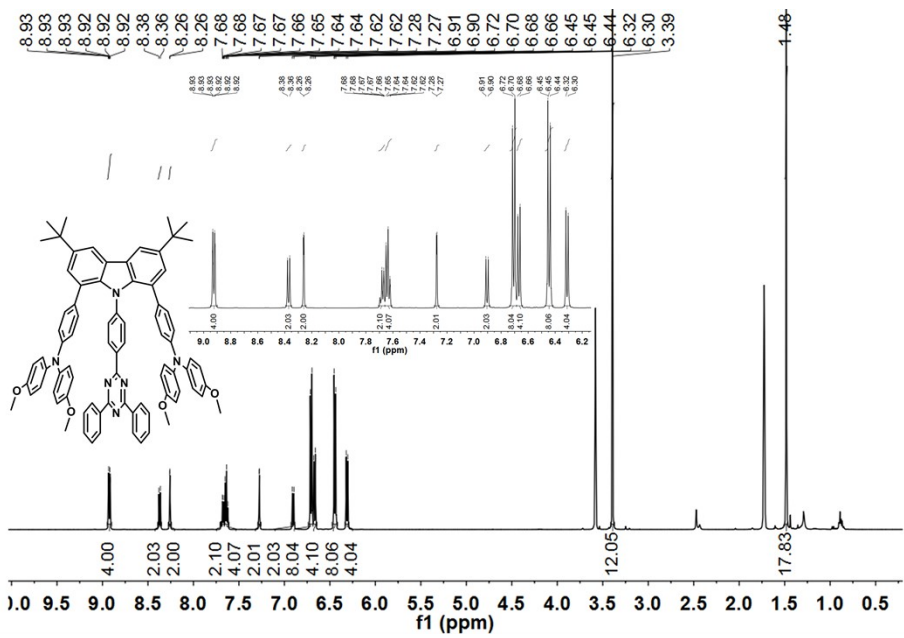


Fig. S19. ¹H NMR spectrum of MPAPTC.

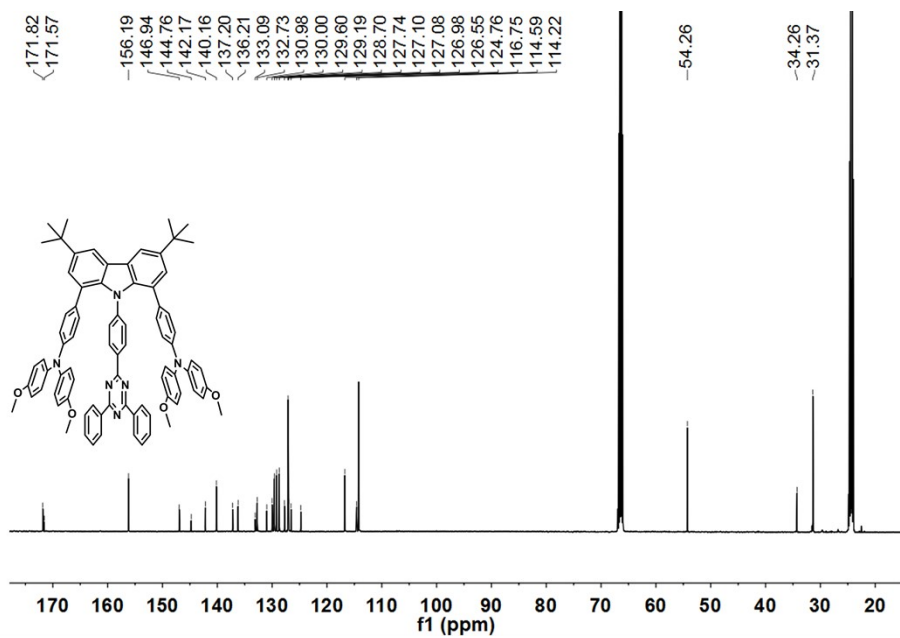


Fig. S20. ^{13}C NMR spectrum of MPAPTC.

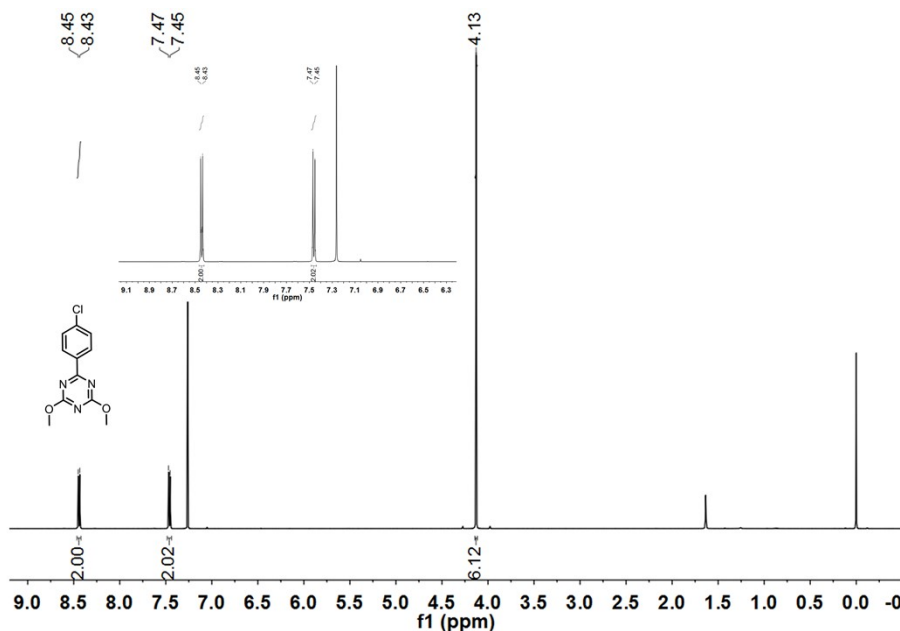


Fig. S21. ^1H NMR spectrum of Cl-MT.

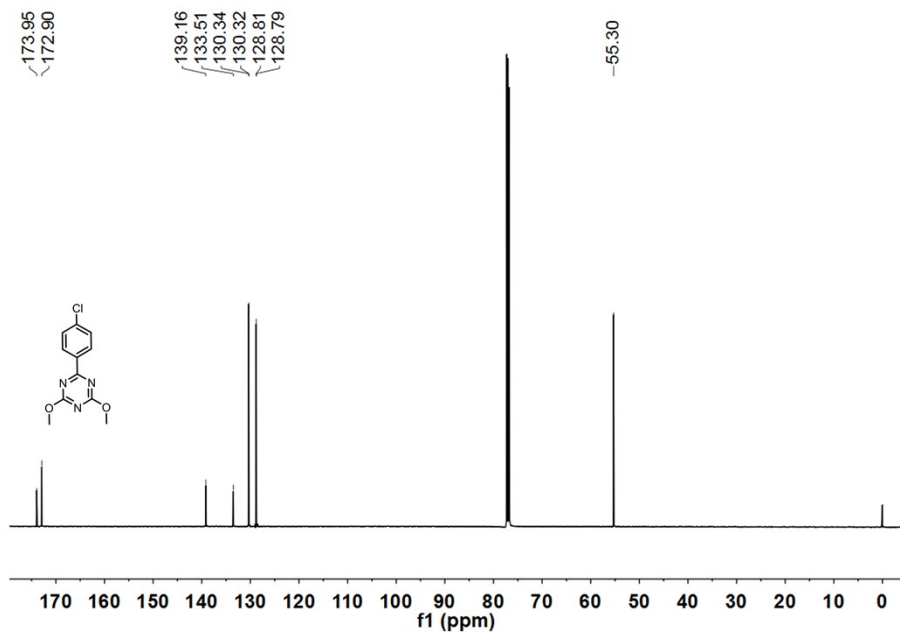


Fig. S22. ^{13}C NMR spectrum of Cl-MT.

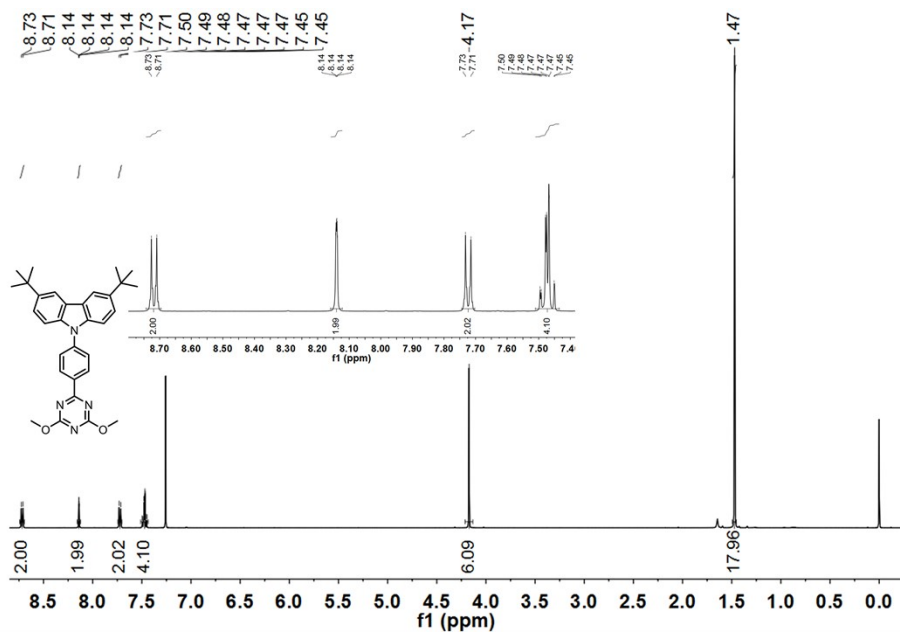


Fig. S23. ^1H NMR spectrum of MTC.

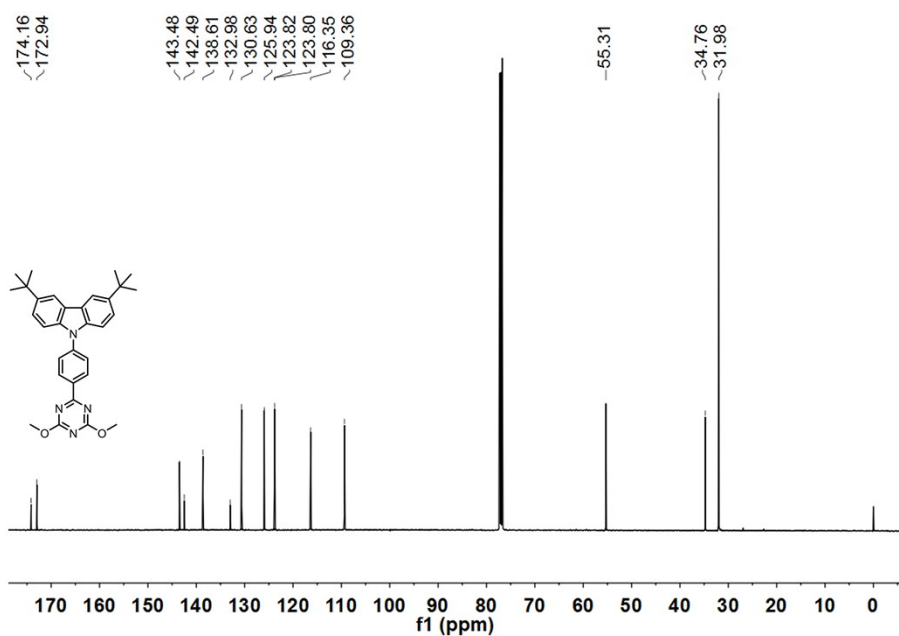


Fig. S24. ^{13}C NMR spectrum of MTC.

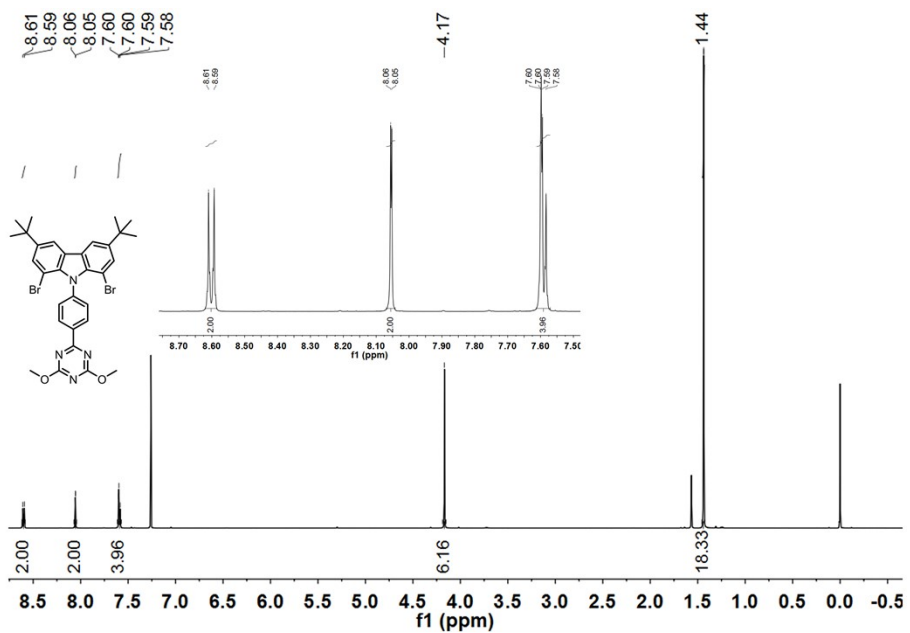


Fig. S25. ^1H NMR spectrum of Br-MTC.

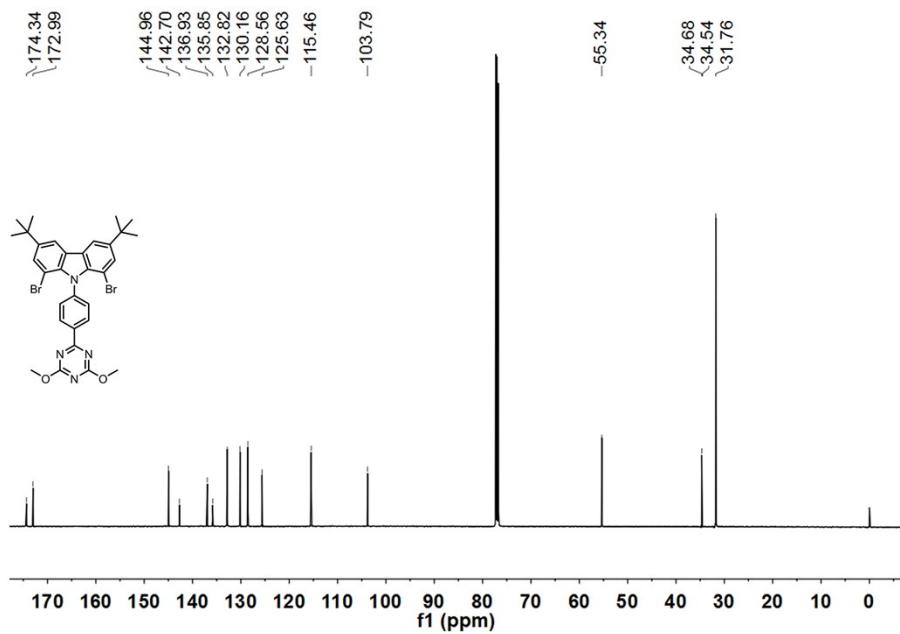


Fig. S26. ^{13}C NMR spectrum of Br-MTC.

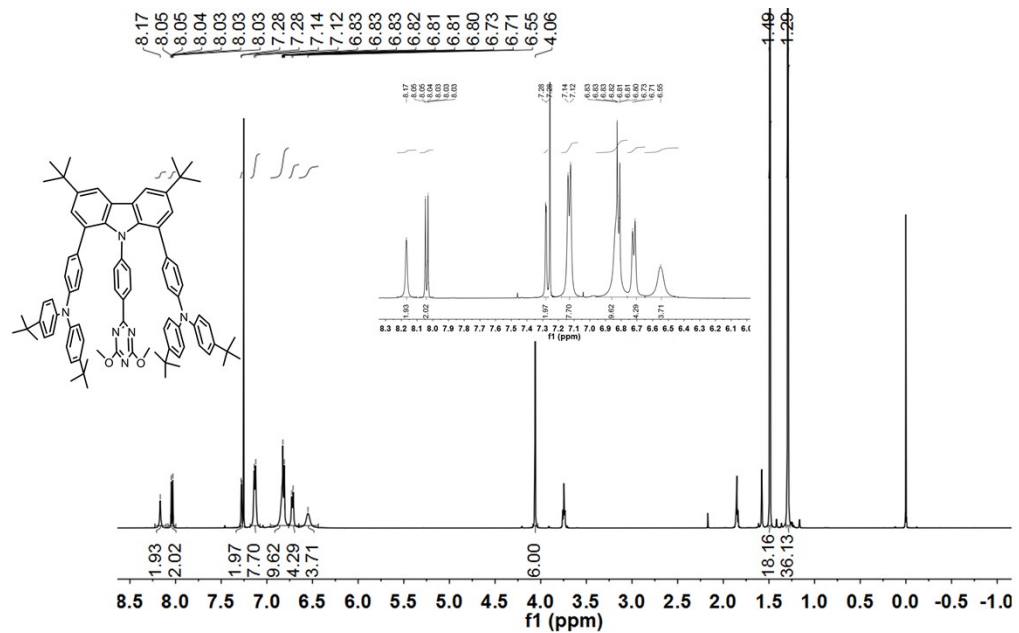


Fig. S27. ^1H NMR spectrum of BPAMTC.

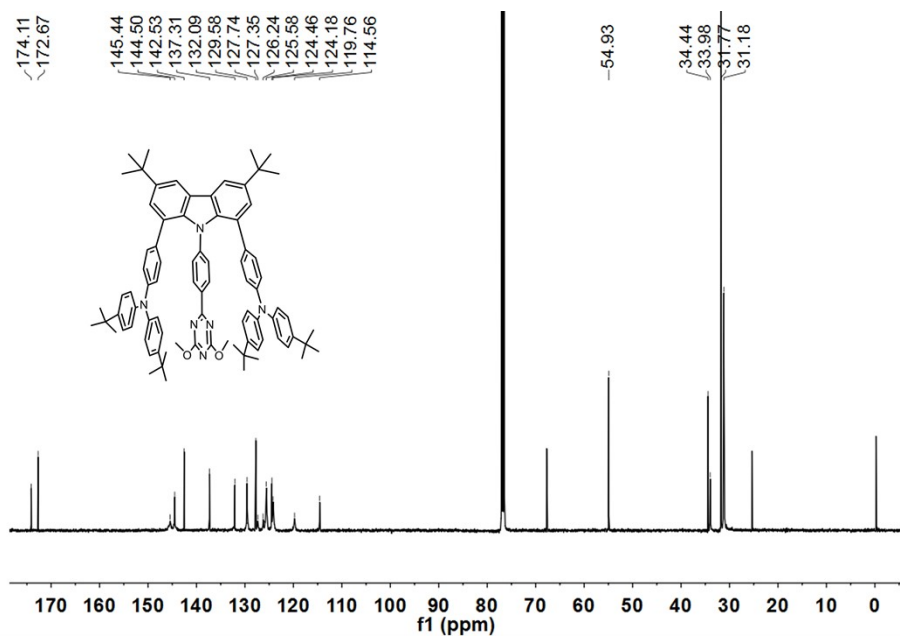


Fig. S28. ^{13}C NMR spectrum of BPAMTC.

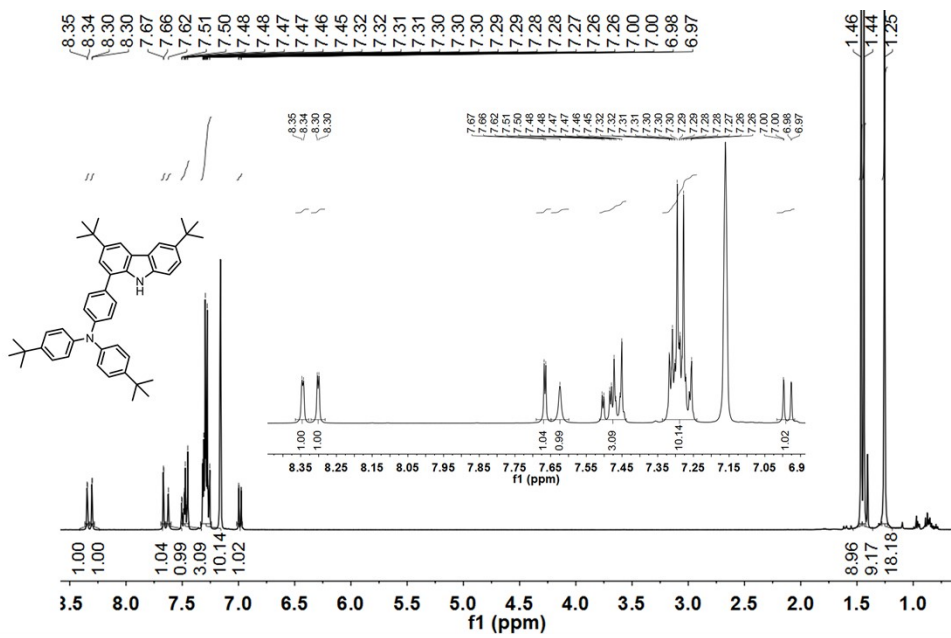


Fig. S29. ^1H NMR spectrum of BPAC.

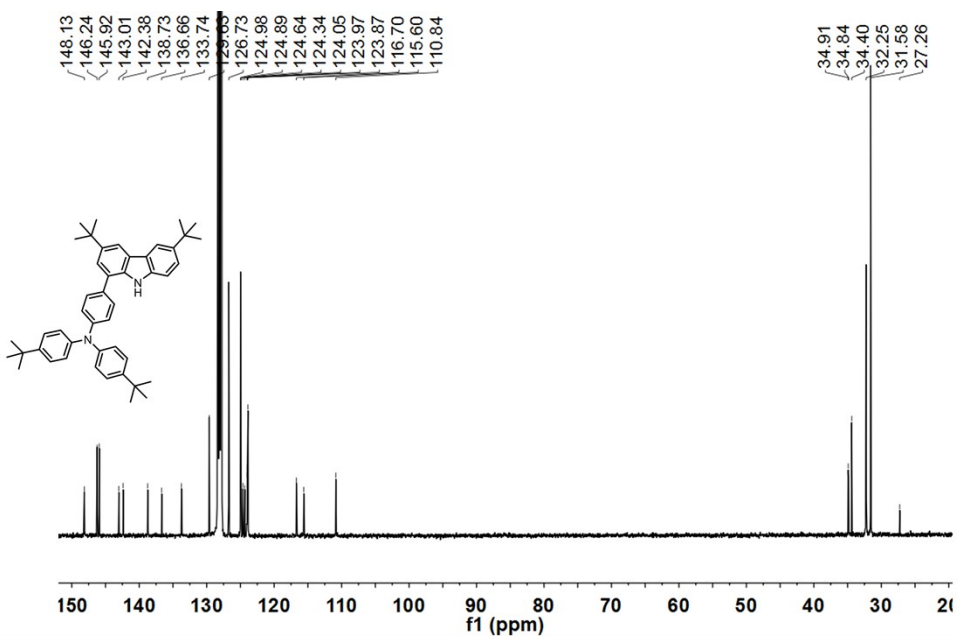


Fig. S30. ^{13}C NMR spectrum of BPAC.

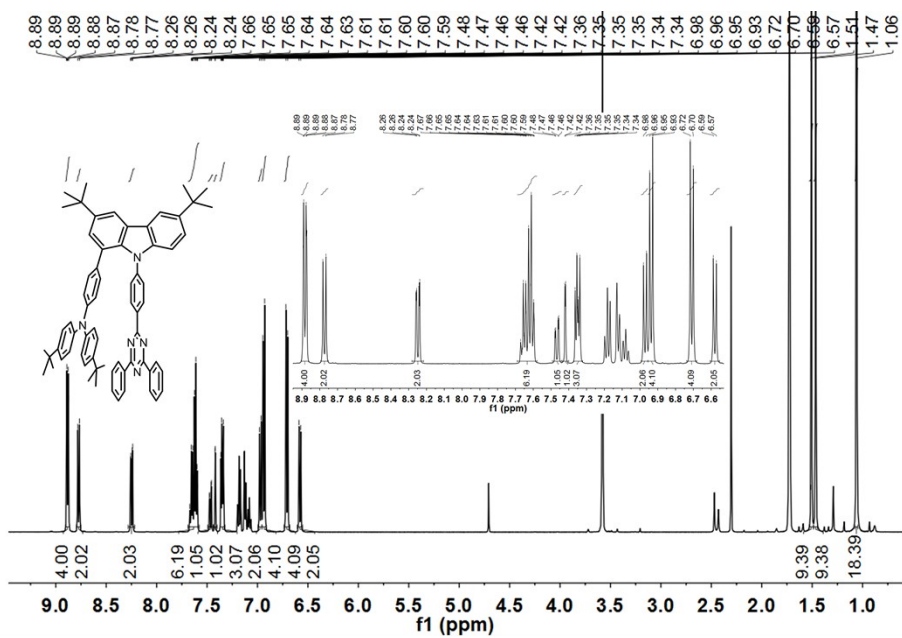


Fig. S31. ^1H NMR spectrum of mBPAPTC.

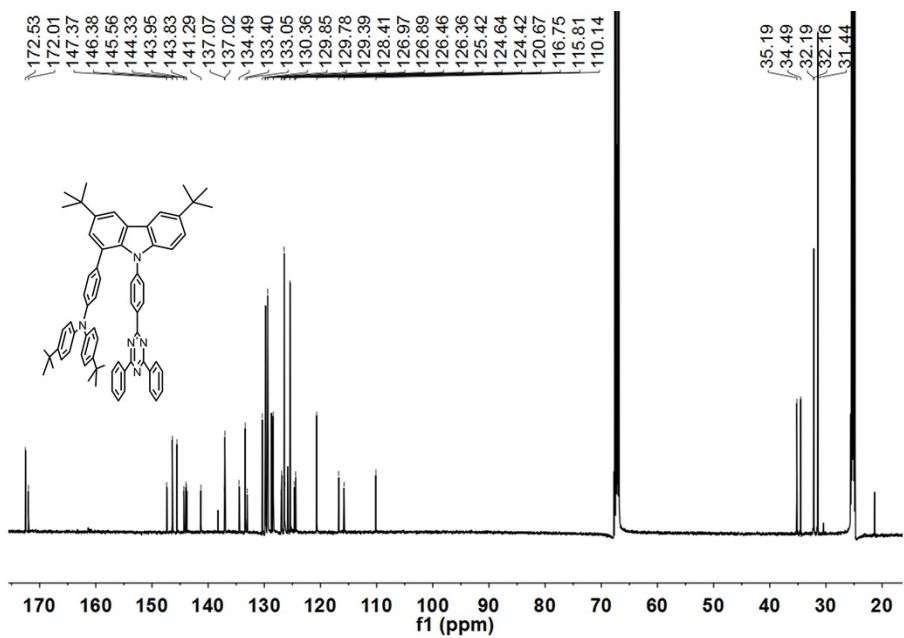


Fig. S32. ^{13}C NMR spectrum of mBPAPTC.

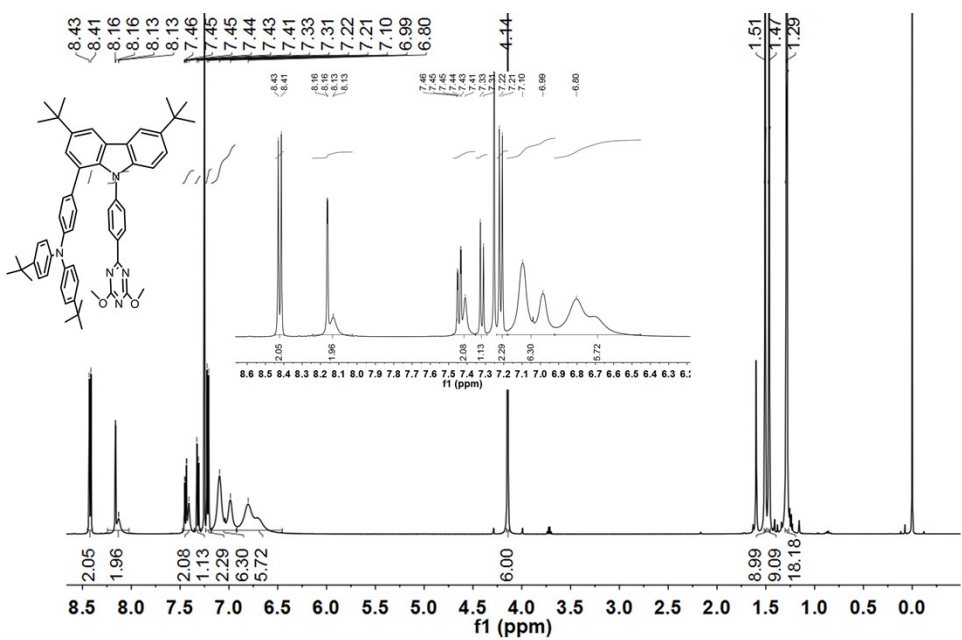


Fig. S33. ^1H NMR spectrum of mBPAMTC.

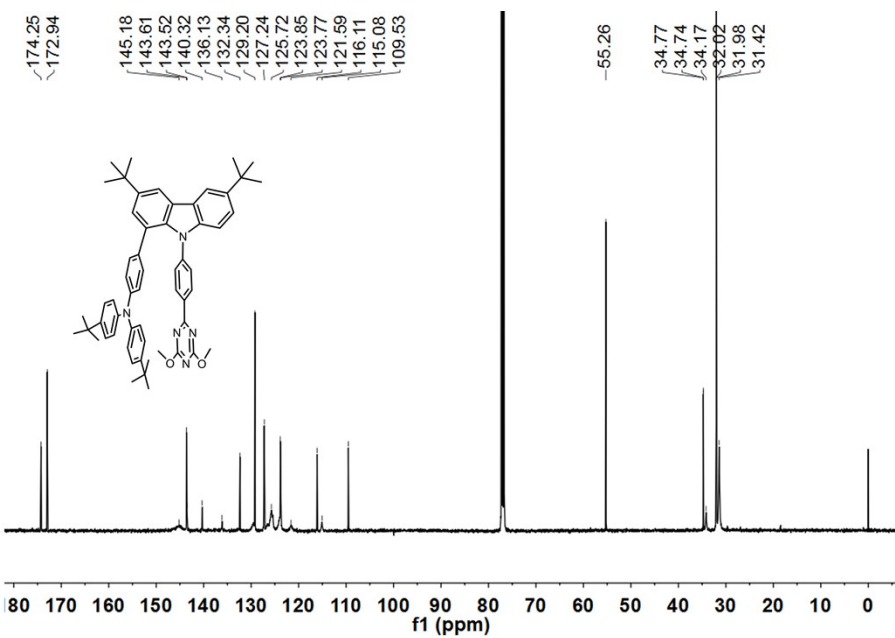


Fig. S34. ¹³C NMR spectrum of mBPAMTC.

References

- [1] H. Tanaka, K. Shizu, H. Miyazaki, C. Adachi, *Chem. Commun.*, 2012, **48**, 11392.
- [2] Y Li, T Tan, S Wang, Y Xiao, X Li, *Dyes Pigments.*, 2017, **144**, 262.
- [3] S Xie, Z Yan, Y Li, Q Song, M Ma, *J. Org. Chem.*, 2018, **83**, 10916.
- [4] P. Pandit, K. Yamamoto, T. Nakamura, K. Nishimura, Y. Kurashige, T. Yanai, G. Nakamura, S. Masaoka, K. Furukawa, Y. Yakiyama, M. Kawano, S. Higashibayashi, *Chem. Sci.*, 2015, **6**, 4160.
- [5] K Li, Y Zhu, B Yao, Y Chen, H Deng, Q Zhang, H Zhan, Z Xie and Y Cheng, *Chem. Commun.*, 2020, **56**, 5957.